Experimental analysis of the brachistochrone using a kinematical approximation method

Enrique Liht and Hans Yang

Science One Program

University of British Columbia

March 2011

Abstract

The solution to the brachistochrone – the curve of fastest descent – for a spherical steel bearing sliding and rolling down a low-friction plastic track is determined from experimental data and numerical analysis. It is hypothesized that the curve of fastest descent will be closely correlated to the cycloid. Analysis involves a spreadsheet simulation of model curves where the times of descent are predicted by an approximation formula derived using basic kinematics. Results display a positive correlation between a model curve's deviation from the cycloid and the time of descent.

Introduction

The original brachistochrone problem asks to find the curve of fastest descent between two points for a sliding body under frictionless conditions. It was first posed and solved in 1696 and 1697 by Johann Bernoulli. He determined that the solution is the cycloid, which is a curve obtained by tracing the trajectory of a single point held on the edge of a circle as the circle rolls one circumference in a straight line [Appendix A]. A compact proof of Bernoulli's proof is presented:

The brachistochrone can be thought of as the path that light will follow through a medium of infinitely thin plates with increasingly higher indices of refraction [1]. According to conservation of energy without dissipative losses, the maximum velocity of an object falling in a constant gravitational field is given by:

$$v_m = \sqrt{2gh} \qquad (1)$$

Where g is a constant gravitational acceleration and h is the height "fallen." The law of refraction gives the following relationship for a beam of light moving through a medium with different indices of refraction:

$$\frac{\sin\theta}{v} = \frac{1}{v}\frac{dx}{ds} = \frac{1}{v_m} \qquad (2)$$

Using equations (1) and (2) we can conclude that the curve of fastest descent is vertical at the starting point where the velocity is zero, and horizontal at the bottom of the curve, where the maximum velocity is reached. Rearranging terms in (2) and squaring gives:

$v_m^2 dx^2 = v^2 ds^2 = v^2(dx^2 + dy^2)$. Solving for dx gives: $dx = \frac{vdy}{\sqrt{v_m^2 - v^2}}$.

Substituting for v and v_m from equations (1) and (2) gives the differential equation of an inverted cycloid generated by a circle of diameter D:

$$dx = \sqrt{\frac{y}{D-y}}\,dy. \qquad (4)$$

Integrating and substituting $x = \frac{1}{2}sin^{-1}\sqrt{\frac{x}{D}} - \sqrt{Dx - x^2}$, we get the Cartesian equation of the cycloid [2]:

$$x = Rcos^{-1}\left(1 - \frac{y}{R}\right) - \sqrt{y(2R - y)}. \qquad (5)$$

Bernoulli's proof is one of many that rely on mathematical rigor to solve the brachistochrone. In this paper, a numerical approach will be presented that aims to defend the cycloid as the solution to the brachistochrone.

Methods

The experimental phase consisted of measuring descent times of a spherical steel bearing rolling down different tracks. All of the tracks were built using hard plastic tubing commonly used for plumbing. These have a coefficient of sliding friction in the range of 0.04-0.5, and a coefficient of rolling friction in the range of 0.001 – 0.005 [3]. Duct tape and tools such as a flat bar, protractor, and tape measurer were used in order to build the curves accurately. A standard stopwatch accurate to milliseconds was used in all measurements.

The first set of experiments comprised of testing the descent times for tracks modeled after the cycloid, the exponential decay curve, and the straight line [Appendix A]. They were drawn with Microsoft Mathematics software, then enlarged, printed, and pasted unto flat wooden boards on which the tracks were glued. However, this method proved inconclusive in that it could only show qualitatively that the cycloid is the fastest curve, and minor alterations to the cycloid only led to descent times that were not significantly different.

A new method was adopted with the idea being that numerous straight segments inclined at different angles would be joined together to form a model curve, and the times of descent could be predicted by using a numerical approach on Microsoft Excel 2007. Hence, the second set of experiments comprises of testing the descent times for straight track segments of length 90.5 cm with angles of inclinations ranging from 10° to 90° at 10° intervals. Note that the model curve is not built physically. Instead, the descent times for the model curves are predicted by a function which that takes into account the velocity picked up in the previous segments. A derivation of this additive time prediction formula follows:

$$Time_{total} = T_1 + \frac{D}{\frac{D}{T_1} + \frac{D}{T_2}} + \frac{D}{\frac{D}{T_1} + \frac{D}{T_2} + \frac{D}{T_3}} + \cdots + \frac{D}{\frac{D}{T_1} + \cdots + \frac{D}{T_n}}$$

$$= T_1 + \frac{D}{\frac{D(T_2 + T_1)}{T_1 T_2}} + \frac{D}{\frac{D(T_2 T_3 + T_1 T_3 + T_1 T_2)}{T_1 T_2 T_3}} + \cdots$$

$$Time_{total} = T_1 + \frac{T_1 T_2}{T_1 + T_2} + \frac{T_1 T_2 T_3}{T_2 T_3 + T_1 T_3 + T_1 T_2} + \cdots \frac{T_1 T_2 \ldots T_n}{T_2 .. T_n + T_1 .. T_3 \ldots + \ldots} \qquad (10)$$

Where T = time (s) measured individually for each straight segment, and D = segment length (m).

This time predicting formula only relies on the individually measured times for each segment. It has a recognizable pattern; in each term, the numerator consists of the product of the individual descent times of the current and previous segments, and the denominator can be thought of as the sum of all the combinations of choosing (n-1) descent times from (n) descent times. This pattern can then be used to derive subsequent terms; the composition of each individual term becomes very complex as the number of segments increases [Appendix B]. In the construction of this formula, the final velocity at a segment was assumed to be equal to the average velocity of that segment. This assumption was justified by the idea that one of the segments is only a small portion of the bigger model curve, so that the small deviations from the actual velocities will not result in significant errors. The results support the use of this assumption.

The model curves all start at the origin (0, 0), and have individual segments of different angles positioned in a way that satisfies the following constraints:

$$0.905 * \sum \cos(\theta_i) = \Delta X = 13.98 \pm 0.2\, m. \qquad (11)$$

$$0.905 * \sum \sin(\theta_i) = \Delta Y = -3.92 \pm 0.2\, m. \qquad (12)$$

Furthermore, a true cycloid is also graphed using the two equations below, and used for comparison.

$$x(y) = \pi cos^{-1}\left(1 - \frac{y}{\pi}\right) - \sqrt{y(2\pi - y)}. \qquad \text{*left half}$$

$$x(y) = -\pi cos^{-1}\left(1 - \frac{y}{\pi}\right) + \sqrt{y(2\pi - y)} + 2\pi^2 - 2.88 \qquad \text{*right half}$$

Where the right half is a reflection of the left half in the y axis and undergoes a horizontal shift to line up with the left half. The point (13.98, -3.92) is found on this cycloid. The model curves are then compared to the cycloid qualitatively by graphical representation and quantitatively by statistical analysis.

Results

Fig. 1: Measured descent times for straight-line segments of length 0.905 meters, with different angles of inclination

Angle (degrees)	Measured Time (s)
90	0.454 ± 0.049
80	0.475 ± 0.044
70	0.498 ± 0.039
60	0.528 ± 0.042
50	0.569 ± 0.035
40	0.621 ± 0.032
30	0.692 ± 0.034
20	0.843 ± 0.027
10	1.252 ± 0.025

The data from this figure represents the time of descent measured for the straight segments of track. Each angle was tested 25 times, and the times are represented with their mean and std. deviation.

Fig. 2: Descent times calculated for the simulated curves built with the straight line segments constrained to an overall length of 13.98 +/- 0.2 m and to an overall height of 3.92 +/- 0.2 m

	Curve # 1	Curve # 2	Curve # 3	Curve # 4	Curve # 5	Curve # 6
Number of straight-line segments	21	20	19	18	17	16
Finishing Position (x, y) in meters	(13.980, -3.920)	(13.866, -3.942)	(13.864, -4.114)	(13.902, -3.855)	(13.859, -3.874)	(13.841, -3.867)
Sequence of straight segments by their angles (degrees)	90 80 70 60 50 40 40 30 30 20 20 10 10 10 -10 -20 -20 -30 -40 -40 -50	90 80 60 60 50 40 30 30 20 20 10 10 10 -10 -10 -20 -30 -30 -40 -40	90 60 50 50 40 40 30 30 20 20 10 10 10 -10 -20 -20 -20 -30 -40	80 60 50 40 30 30 20 20 20 10 10 10 -10 -10 -10 -20 -20 -20	60 50 40 40 30 20 10 10 10 10 10 10 10 -10 -10 -10 -10	30 30 20 20 20 20 20 10 10 10 10 10 10 10 10 10
Simulated overall time (s)	2.136	2.091	2.077	2.149	2.230	2.594

This figure shows the data compiled from the model using equations (8), (9), and (10). The curves have different number of straight segments, because they differ in length due to their unique curvatures. All of the curves are measured in meters, start at the point (0,0), and end at (13.98, 3.92) with an uncertainty of $\pm$ 0.2. The uncertainty is due to the fact that up to 21 straight segments are used in order to build a constrained curve. The sequence of angles is interpreted as the sequence of straight segments that make up the overall curve, and are read from (0,0) to the end point of each curve.. Also note that the negative angles represent segments for which the bearing is ascending; in this case, the times for such segments are taken to be negative, so that in the time predicting formula, it translates into a negative velocity being added on to previous velocities.

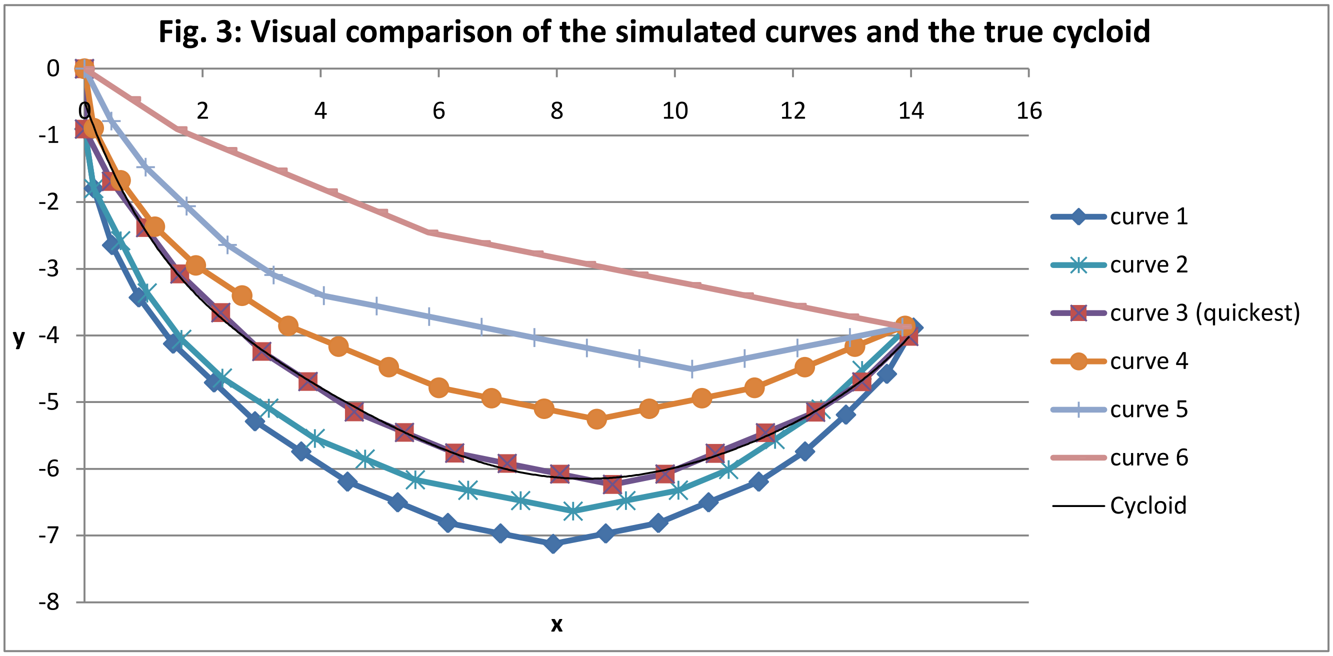

Fig.3 shows the curves obtained from the model. The thin black line represents the true cycloid. The curve of fastest descent is curve 3, and is almost identical to the cycloid. All of the other curves, which are either above or below curve 3 are slower. The statistical analysis of the curves is presented in the discussion.

Discussion

In order to show that the cycloid is the fastest curve, we show that the times of descent increase for curves as they deviate from the shape of the cycloid.

Analyzing the brachistochrone in a realistic setting means having to deal with friction and rolling motion, which make an analytical approach to the problem much more complex. Our approach used experimental data in order to determine to a certain level of accuracy whether the curve of fastest descent in a realistic setting is the cycloid.

The initial attempt to measure descent times for tracks of various shapes and reasonable size proved to be inadequate because the descent times for similar curves were nearly indistinguishable using the millisecond stopwatch. Hence, this inspired the kinematical approximation of a segmented model curve as a means of analyzing the brachistochrone from a new perspective.

The model used an assumption that the average velocity of the metal bearing down any single straight segment was equal to its final velocity after that particular segment. The assumption seemed quite significant at the beginning, but the data showed that within our size constraints, 16 straight track segments were enough to produce good curves. The curve of fastest descent was achieved with 19 segments, and when comparing it to the true cycloid, it is evident that the assumption worked well, and the model has predictive power.

In order to support the hypothesis that the fastest curve will be cycloid-like, a model curve is simulated so that each composing straight segment closely follows the trajectory of a cycloid. Subsequently, by using extra segments, two other model curves that went below the trajectory of the cycloid were simulated. In addition, by using less segments, three model curves that went above the trajectory of the cycloid were simulated.

Calculations from the time prediction formula show that the curve modelled after the cycloid had the shortest descent time. These results support the hypothesis that the curve of fastest descent is almost identical to the cycloid. Well-known analytic mathematical models for the brachistochrone with friction [2],[4],[5], predict that under low coefficients of friction, the curve of fastest descent will be extremely similar to the cycloid, and our data supports their findings.

Having shown that the cycloid is the curve of fastest descent using our experimental data and numerical model, we quantified the similarities between each of the curves to the true cycloid using the S = (Sum of Squared Differences method) = $\sum_y^N (model_y - cycloid_y)^2$. We found very low S values for the curves which were very similar to the cycloid.

We then plotted each of the simulated curve's overall descent time against their S values, and found a very strong linear correlation shown in Figure 4.

Figure 4: Relationship between descent time and resemblance of a curve to the cycloid as measured by the summed squared differences method

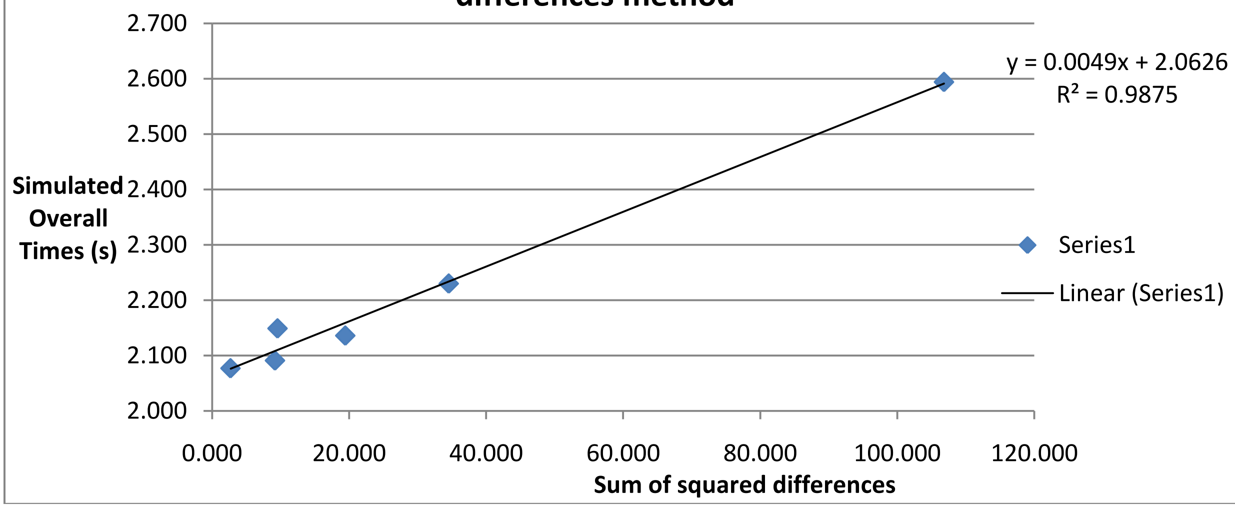

Fig. 4 quantitatively displays the relationship between a curve's resemblances to the cycloid and its descent time. The resemblance of the curves to the cycloid was measured using $Sum\ of\ squared\ differences = S = \sum_y^N (model_y - cycloid_y)^2$. A larger value for the sum of squared differences translates into less resemblance to the true cycloid.

It is clear that the overall descent time for a steel ball-bearing on our curves can be predicted from the curve's resemblance to the cycloid as measured by the Sum of Squared differences method (S). It appears that this relationship can be then extrapolated to predict descent times for tracks with different shapes as long as the following circumstances are met:

i) A cycloidal curve is the curve of fastest descent for the specific level of friction in that track.
ii) The curves being compared are continuous, differentiable everywhere, and have a constant change in slope.

We believe that some inconsistencies in our data are due to oversimplifying assumptions of the actual motion of the bearing. We assumed in our theoretical calculations that the steel bearing descends by rolling and encounters rolling friction. However, due to the steepness of the cycloid (or steep straight segments), the bearing may actually descend by a combination of sliding and rolling motion. Other errors can be attributed to the inaccuracy of the timing method, which we attempted to mitigate with more trials and longer track segments.

It is important to note that the derived kinematical time prediction formula (10) is only an approximation. It has nonetheless proven to be more reliable than measuring descent times for actual model curves of reasonable size. It is recommended that if adequate computing is available, that the time prediction formula should be modified by including more segments of smaller length so that the approximation becomes analogous to taking a line integral.

Conclusion

A strong positive correlation was found between the curves' deviation from the cycloid (measured by the summed squared differences method) and the descent times. Our experiment supports the hypothesis and the literature that the cycloid minimizes descent time for low-friction settings. Future experiments utilizing similar methods as presented can improve upon these results by simulating model curves constituted by more but shorter segments. Such numerical endeavours to determine the solution to the brachistochrone will be a great augmentation to the mathematical proof behind this elegant problem.

Bibliography

[1] Erlichson, H. Johnann Bernoulli's brachistochrone solution using Fermat's principle of least time. European Journal of Physics, 20: 299 (1999).

[2] Haws, L., Kiser, T. Exploring the Brachistochrone Problem. The American Mathematical Monthly, 102: 4, 328 (1995).

[3] Avallone, E.A., Baumeister, T. Mark's Standard Handbook for Mechanical Engineers; 10th ed. McGraw-Hill Professional (1996).

[4] Ashby, N., Brittin, W.E., Love, W.F., Wyss, W. Brachistochrone with Coulomb friction. American Journal of Physics, 43: 10, 902 (1975).

[5] Negron-Marrero, P.V., Santiago-Figueroa, B.L. The Nonlinear Brachistochrone Problem with Friction. Dept. Mathematics, University of Puerto Rico Humacao. http://mate.uprh.edu/~urmaa/reports/brach.pdf. (2005).

[6] Lawlor, G., A New minimization proof for the Brachistochrone. The American Mathematical Monthly, 103: 3, 242 (1996).

Appendix A

Fig. 5: Creating a cycloid by tracing a point on the edge of a rolling circle

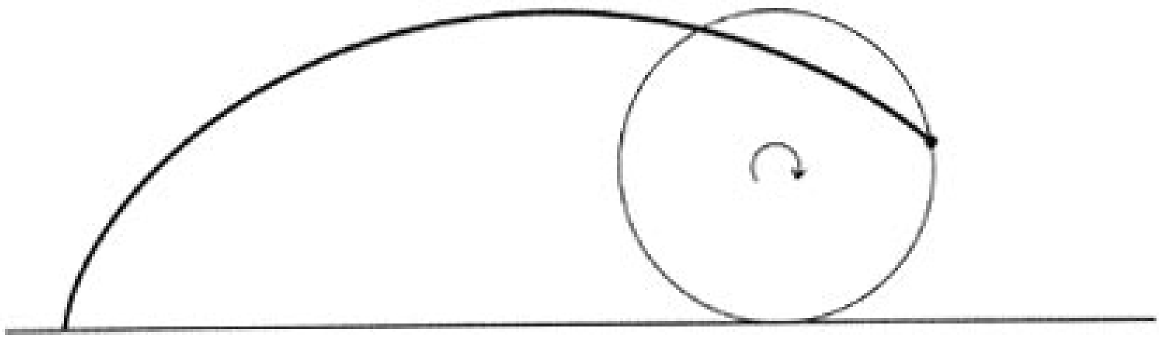

Fig. 5 was obtained without permission from [6].

Fig. 6: On the left; a picture of the straight-line track segment used at different angles for the model, and an exponential curve used for comparisons. On the right; A scaled down cycloid used for comparisons.

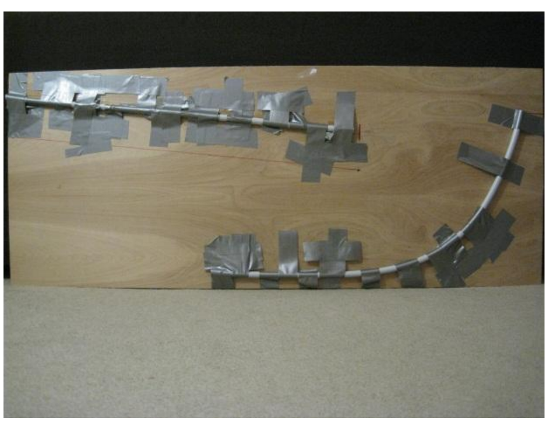

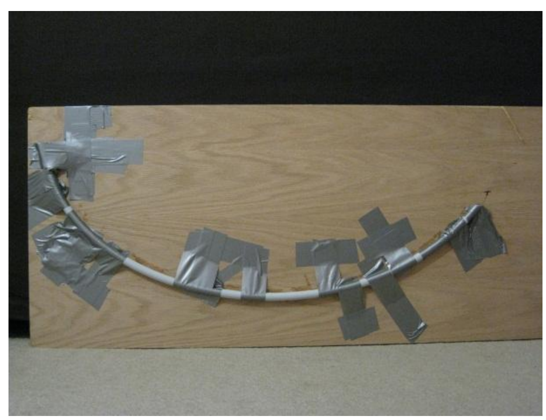

Appendix B

Fig. 5: Screenshot of the Spreadsheet used to compute overall times.

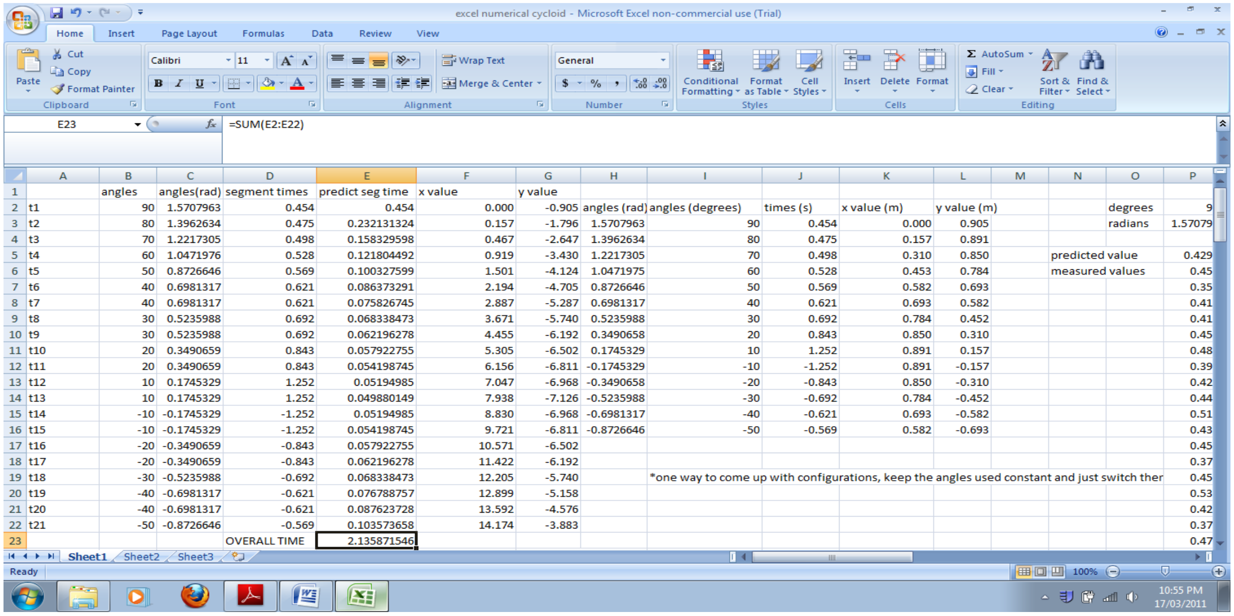

E23 =SUM(E2:E22)

	A	B	C	D	E	F	G
1		angles	angles(rad)	segment times	predict seg time	x value	y value
2	t1	90	1.5707963	0.454	0.454	0.000	-0.905
3	t2	80	1.3962634	0.475	0.232131324	0.157	-1.796
4	t3	70	1.2217305	0.498	0.158329598	0.467	-2.647
5	t4	60	1.0471976	0.528	0.121804492	0.919	-3.430
6	t5	50	0.8726646	0.569	0.100327599	1.501	-4.124
7	t6	40	0.6981317	0.621	0.086373291	2.194	-4.705
8	t7	40	0.6981317	0.621	0.075826745	2.887	-5.287
9	t8	30	0.5235988	0.692	0.068338473	3.671	-5.740
10	t9	30	0.5235988	0.692	0.062196278	4.455	-6.192
11	t10	20	0.3490659	0.843	0.057922755	5.305	-6.502
12	t11	20	0.3490659	0.843	0.054198745	6.156	-6.811
13	t12	10	0.1745329	1.252	0.05194985	7.047	-6.968
14	t13	10	0.1745329	1.252	0.049880149	7.938	-7.126
15	t14	-10	-0.1745329	-1.252	0.05194985	8.830	-6.968
16	t15	-10	-0.1745329	-1.252	0.054198745	9.721	-6.811
17	t16	-20	-0.3490659	-0.843	0.057922755	10.571	-6.502
18	t17	-20	-0.3490659	-0.843	0.062196278	11.422	-6.192
19	t18	-30	-0.5235988	-0.692	0.068338473	12.205	-5.740
20	t19	-40	-0.6981317	-0.621	0.076788757	12.899	-5.158
21	t20	-40	-0.6981317	-0.621	0.087623728	13.592	-4.576
22	t21	-50	-0.8726646	-0.569	0.103573658	14.174	-3.883
23				OVERALL TIME	2.135871546		

	H	I	J	K	L	M	N	O	P
1									
2	angles (rad)	angles (degrees)	times (s)	x value (m)	y value (m)			degrees	9
3	1.5707963	90	0.454	0.000	0.905			radians	1.57079
4	1.3962634	80	0.475	0.157	0.891				
5	1.2217305	70	0.498	0.310	0.850		predicted value		0.429
6	1.0471975	60	0.528	0.453	0.784		measured values		0.45
7	0.8726646	50	0.569	0.582	0.693				0.35
8	0.6981317	40	0.621	0.693	0.582				0.41
9	0.5235988	30	0.692	0.784	0.452				0.41
10	0.3490658	20	0.843	0.850	0.310				0.45
11	0.1745329	10	1.252	0.891	0.157				0.48
12	-0.1745329	-10	-1.252	0.891	-0.157				0.39
13	-0.3490658	-20	-0.843	0.850	-0.310				0.42
14	-0.5235988	-30	-0.692	0.784	-0.452				0.44
15	-0.6981317	-40	-0.621	0.693	-0.582				0.51
16	-0.8726646	-50	-0.569	0.582	-0.693				0.43
17									0.45
18									0.37
19		*one way to come up with configurations, keep the angles used constant and just switch ther							0.45
20									0.53
21									0.42
22									0.37
23									0.47

Fig. 6: Part of the time prediction formula (10) showing the calculation performed to compute the descent time for a single straight track segment placed at the end of curve 1 (segment # 21). This shows how complicated the calculation becomes as the number of track segments increase

D2*D3*D4*D5*D6*D7*D8*D9*D10*D11*D12*D13*D14*D15*D16*D17*D18*D19*D20*D21*D22/(D2*D3*D4*D5*D6*D7*D8*D9*D10*D11*D12*D13*D14*D15*D16*D17*D18*D19*D20*D21+D2*D3*D4*D5*D6*D7*D8*D9*D10*D11*D12*D13*D14*D15*D16*D17*D18*D19*D20*D22+D2*D3*D4*D5*D6*D7*D8*D9*D10*D11*D12*D13*D14*D15*D16*D17*D18*D19*D21*D22+D2*D3*D4*D5*D6*D7*D8*D9*D10*D11*D12*D13*D14*D15*D16*D17*D18*D20*D21*D22+D2*D3*D4*D5*D6*D7*D8*D9*D10*D11*D12*D13*D14*D15*D16*D17*D19*D20*D21*D22+D2*D3*D4*D5*D6*D7*D8*D9*D10*D11*D12*D13*D14*D15*D16*D18*D19*D20*D21*D22+D2*D3*D4*D5*D6*D7*D8*D9*D10*D11*D12*D13*D14*D15*D17*D18*D19*D20*D21*D22+D2*D3*D4*D5*D6*D7*D8*D9*D10*D11*D12*D13*D14*D16*D17*D18*D19*D20*D21*D22+D2*D3*D4*D5*D6*D7*D8*D9*D10*D11*D12*D13*D15*D16*D17*D18*D19*D20*D21*D22+D2*D3*D4*D5*D6*D7*D8*D9*D10*D11*D12*D14*D15*D16*D17*D18*D19*D20*D21*D22+D2*D3*D4*D5*D6*D7*D8*D9*D10*D11*D13*D14*D15*D16*D17*D18*D19*D20*D21*D22+D2*D3*D4*D5*D6*D7*D8*D9*D10*D12*D13*D14*D15*D16*D17*D18*D19*D20*D21*D22+D2*D3*D4*D5*D6*D7*D8*D9*D11*D12*D13*D14*D15*D16*D17*D18*D19*D20*D21*D22+D2*D3*D4*D5*D6*D7*D8*D10*D11*D12*D13*D14*D15*D16*D17*D18*D19*D20*D21*D22+D2*D3*D4*D5*D6*D7*D9*D10*D11*D12*D13*D14*D15*D16*D17*D18*D19*D20*D21*D22+D2*D3*D4*D5*D6*D8*D9*D10*D11*D12*D13*D14*D15*D16*D17*D18*D19*D20*D21*D22+D2*D3*D4*D5*D7*D8*D9*D10*D11*D12*D13*D14*D15*D16*D17*D18*D19*D20*D21*D22+D2*D3*D4*D6*D7*D8*D9*D10*D11*D12*D13*D14*D15*D16*D17*D18*D19*D20*D21*D22+D2*D3*D5*D6*D7*D8*D9*D10*D11*D12*D13*D14*D15*D16*D17*D18*D19*D20*D21*D22+D2*D4*D5*D6*D7*D8*D9*D10*D11*D12*D13*D14*D15*D16*D17*D18*D19*D20*D21*D22+D3*D4*D5*D6*D7*D8*D9*D10*D11*D12*D13*D14*D15*D16*D17*D18*D19*D20*D21*D22